

## Observation of Coulomb Focusing of Autoionization Electrons Produced in Low-Energy $\text{He}^+ + \text{He}$ Collisions

J. K. Swenson,<sup>(a)</sup> C. C. Havener, N. Stolterfoht,<sup>(b)</sup> K. Sommer,<sup>(b)</sup> and F. W. Meyer

*Oak Ridge National Laboratory, Oak Ridge, Tennessee 37831-6372*

(Received 13 February 1989)

We report observation of a significant enhancement in the intensity of target and projectile autoionizing electrons produced in low-energy (2–15-keV)  $\text{He}^+ + \text{He}$  collisions. The target electron intensity is strongly peaked at  $0^\circ$  and confined to an angular range of  $\approx 5^\circ$  about the incident beam direction, while the projectile electron intensity shows a similar enhancement at  $180^\circ$ . We attribute this effect to *Coulomb focusing*, a new aspect of post-collision interaction which results from the deflection of the ejected electrons in the Coulomb field of the receding spectator ion.

PACS numbers: 34.70.+e, 34.50.Fa

When autoionizing states formed in low-energy ion-atom collisions decay in the proximity of the receding spectator ion, the ejected electron's energy is reduced by the attractive Coulomb potential of the ion, resulting in a broadened spectral line shape whose maximum is shifted towards lower electron energies. Barker and Berry<sup>1</sup> first observed this post-collision interaction (PCI) effect in ion-atom collisions and presented a model which successfully described the features present in their data. Their treatment, however, did not take into account the relative motion of the ion during the time the electron takes to emerge from the interaction region. In extending this model to electron-atom collisions, Ogurtsov<sup>2</sup> accounted for the finite interaction time between the Auger electron and the slowly receding scattered electron. More recently, Arcuni<sup>3</sup> and van der Straten and Morgenstern<sup>4</sup> applied this idea to ion-atom collisions, and derived expressions for emission-angle-dependent kinematic corrections to the PCI line shape, which result from the deflection of the electron in the Coulomb field of the spectator ion. Other authors have suggested that, for electron velocities greater than that of the ion, the post-collision deflection of electrons ejected close to the collision axis can result in Doppler broadening of the PCI line shape,<sup>5,6</sup> and cause a redistribution of the electron intensity in this region.<sup>7</sup> In addition, it has been speculated that these effects may also be important in collisions where the ejected velocity is less than that of the ion.<sup>8</sup> For attractive potentials (i.e., for positively charged ions), the deflection effectively *compresses* the emitter-frame solid angle, resulting in an enhancement, or *focusing*, of electron intensity in the direction of the ion. This effect, which is referred to as *Coulomb focusing*, has not previously been identified in ion-atom collision experiments.

In this Letter, we present the first experimental measurements which show conclusive evidence for Coulomb focusing in ion-atom collisions. Using the technique of high-resolution zero-degree electron spectroscopy, we measured the energy spectra of autoionizing electrons emitted following 2–15-keV  $\text{He}^+ + \text{He}$  collisions. For

10-keV collisions, we observe a fourfold enhancement in the total intensity of electrons emitted from target and projectile autoionizing states for observation angles of  $0^\circ$  and  $180^\circ$ , respectively. Measurements of the angular distribution of these electrons about the forward direction show that the enhancement is strongly peaked at  $0^\circ$  and confined to an angular range of  $\approx 5^\circ$  about the incident beam axis. The enhancement is observed to increase with decreasing lifetime of the autoionizing state and with increasing collision energy. We present a simple classical time-dependent treatment of post-collision interaction which models the deflection of the ejected electron in the field of the spectator ion and gives good quantitative agreement with the experimental data. Our results show that for collision energies above about 5 keV, Coulomb focusing can be the most significant consequence of PCI in electron-energy spectra measured along the ion-beam direction.

The measurements were performed at the Oak Ridge National Laboratory electron cyclotron resonance ion-source facility using a tandem electron spectrometer temporarily transported from the Hahn-Meitner Institut. Target and projectile Auger electrons emitted following 2–15-keV  $\text{He}^+ + \text{He}$  collisions were detected at observation angles ranging from  $0^\circ$  to  $30^\circ$ , and (for 10 keV) at  $180^\circ$  relative to the ion-beam direction. The experimental arrangement used for the  $0^\circ$  and  $180^\circ$  measurements, which includes a 5-cm gas target cell, has been described previously.<sup>9</sup> A gas jet target was used for the off-axis measurements. Target pressures of less than  $1 \times 10^{-3}$  Torr were used to insure single-collision conditions.

The dominant mechanism through which autoionizing states are formed in low-energy ( $v_p < 0.5$  a.u.) collisions is electron promotion. For symmetric systems such as  $\text{He}^+ + \text{He}$ , this mechanism populates singlet autoionizing states with equal probability in either the target or projectile.<sup>10</sup> Indeed, Brodenave-Montesquieu, Gleizes, and Benoit-Cattin<sup>11</sup> have shown that for the collision energy range 10 to 30 keV and for emission angles ranging from  $20^\circ$  to  $160^\circ$ , electron emission from equivalent tar-

get and projectile autoionizing states is characterized by identical differential cross sections which are symmetric about  $90^\circ$  in the center-of-mass frame (i.e., independent of the relative position of the charged collision partner). In contrast, for a small range of emission angles about  $0^\circ$  and  $180^\circ$ , we measure a strong enhancement of autoionization electron intensity in the direction of the charged collision partner, indicating a significantly *asymmetric* differential cross section.

Figure 1 shows laboratory-frame electron-energy spectra measured at  $0^\circ$  and  $180^\circ$  relative to the incident beam axis for 10-keV  $\text{He}^+ + \text{He}$  collisions. Target autoionizing transitions are denoted  $T$  and occur between 30 and 40 eV in both spectra. The corresponding transitions in the projectile, denoted  $P$ , are Doppler shifted in energy relative to the target transitions, appearing in the energy range 47–57 and 18–28 eV in the  $0^\circ$  and  $180^\circ$  spectra, respectively. After the appropriate kinematical corrections,<sup>12</sup> we determine a ratio in the total target-to-projectile autoionizing electron cross section at  $0^\circ$  of  $\sigma_T/\sigma_P = 4.1 \pm 0.2$  and a projectile-to-target cross-section ratio of  $\sigma_P/\sigma_T = 3.6 \pm 0.3$  at  $180^\circ$ .

Relative cross sections were also determined for individual autoionizing states comprising the total electron emission. Figure 2 shows the measured target-to-projectile cross-section ratios  $\sigma_T^i/\sigma_P^j$  for the singlet states (labeled  $a-e$ ) in the  $0^\circ$  spectrum of Fig. 1, plotted versus the lifetime  $\tau$  of the state.<sup>13</sup> The  $2s^2\ ^1S$  state, which has the shortest lifetime [ $\tau = (4.8 \pm 0.5) \times 10^{-15}$  sec], exhibits the largest enhancement. For this state we determine the ratio  $\sigma_T^i/\sigma_P^j$  to be  $7.9 \pm 0.9$  at 10 keV and  $12 \pm 5$  at 15 keV, corresponding to over an *order-of-magnitude* enhancement in intensity. As can be seen from the figure, the cross-section ratio shows a strong dependence on lifetime, decreasing sharply with increas-

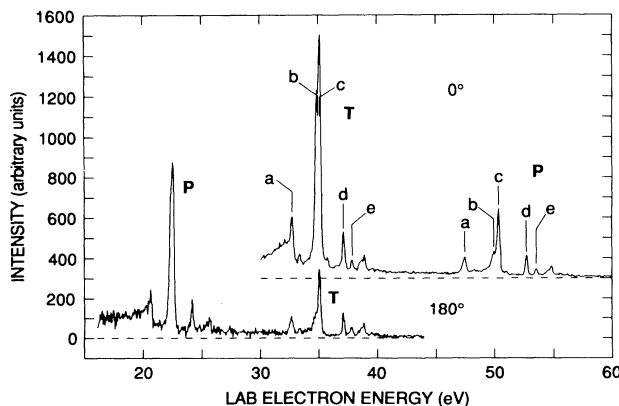


FIG. 1. Laboratory-frame electron-energy spectra measured for 10-keV  $\text{He}^+ + \text{He}$  collisions at  $0^\circ$  and  $180^\circ$  observation angles. Target and projectile autoionization groups are denoted  $T$  and  $P$ , respectively. Individual autoionizing line assignments are (a)  $2s^2\ ^1S$ , (b)  $2p^2\ ^1D$ , (c)  $2s2p\ ^1P$ , (d)  $2p^2\ ^1S$ , and (e)  $2s3s\ ^1S$ .

ing lifetime of the autoionizing state. The apparent disagreement between the enhancement measured for the  $2s3s\ ^1S$  state and the trend established by the rest of the data is not understood at present.

The measured angular variation in the total target-to-projectile cross-section ratio  $\sigma_T/\sigma_P$  is shown in Fig. 3 for the collision energies studied. Directing attention to the 10-keV data represented by the solid circles, one sees that the ratio maximizes at  $0^\circ$  and falls off sharply with observation angle. At  $30^\circ$  the enhancement is gone, and comes into agreement with the predictions of the electron-promotion model and with previous measurements.<sup>11</sup> As can be seen, the 5- and 15-keV data show a similar angular dependence out to  $5^\circ$ . The enhancement is found to be strongest for the 15-keV data and decreases with decreasing collision energy.

We interpret the observed enhancement in the target and projectile electron cross sections at  $0^\circ$  and  $180^\circ$ , respectively, as well as its dependence upon observation angle and autoionizing lifetime, as direct evidence for Coulomb focusing in these low-energy collisions. Based on the conceptual model discussed above, Coulomb focusing will depend upon the strength of the ion's field at the time of electron emission and the path the electron takes through that field. Thus, we expect to see the greatest effect for target and projectile autoionizing states having the shortest lifetimes, and for emission angles in the direction of the ion. The effects of Coulomb focusing should also decrease with increasing collision energy as well as autoionizing transition energy. However, the observed collision energy dependence is opposite to the expected behavior. This apparent discrepancy is resolved by taking into account the small-angle scatter-

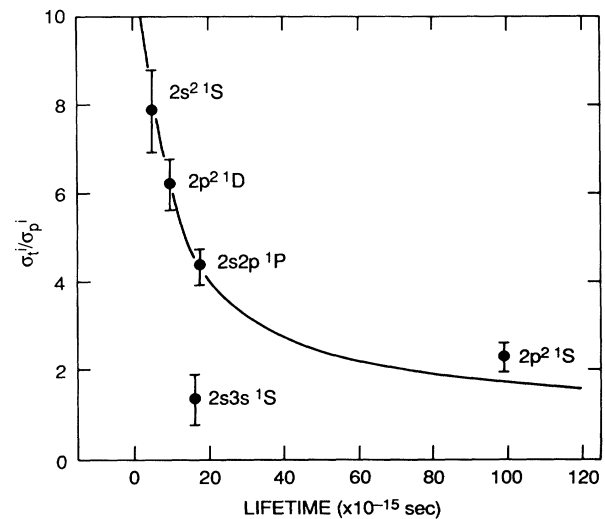


FIG. 2. Ratio of cross section  $\sigma_T^i/\sigma_P^j$  for the individual autoionizing states, indicated in the  $0^\circ$  spectrum of Fig. 1, plotted vs lifetime  $\tau$ . The solid curve is the calculated lifetime dependence for Coulomb focusing (see text).

ing of the  $\text{He}^+$  projectiles during the collision,<sup>14</sup> which tends to distribute the total enhancement over a progressively larger range of emission angles as the collision energy decreases.

To aid in a more quantitative interpretation of the observed features in the data, we present a classical time-dependent treatment of PCI, from which we obtain an emitter-frame cross section, differential in energy and angle, that represents the PCI line shape including

$$\frac{d^2\sigma}{d\Omega dE} = \frac{d\sigma}{d\Delta} \left( \frac{q\Gamma \exp(-q\Gamma/v_p \Delta E')}{v_p \Delta E'^2} \right) \left\{ \frac{\epsilon'}{\epsilon_r} \left[ \frac{E}{E'} \left( 1 - \frac{\epsilon_p}{\epsilon_r} \sin^2 \delta' \right) \right]^{1/2} \right\} \frac{d\Delta'}{d\Omega'}, \quad (1)$$

where the relation is evaluated at the resonance energy  $\epsilon = \epsilon_r$ , and  $\epsilon_p = v_p^2/2$  is the reduced ion energy.<sup>12</sup> The variables  $\Delta, \epsilon, \delta$  and  $\Omega, E, \theta$  are the emitter-frame solid angle, electron energy, and emission angle before and after scattering, respectively. Corresponding *primed* variables refer to these same quantities evaluated in the focusing ion's reference frame and are related via the collision kinematics.<sup>12</sup> The variable  $\Delta E' = \epsilon' - E' = q/R$  is the energy shift experienced by the electron in the ion frame as it emerges from the Coulomb field of the ion.

The above relation represents a Barker-Berry<sup>1</sup>-type broadened line shape modified by terms resulting from a change in the variable of integration and from kinematic transformations<sup>12</sup> to and from the ion frame before and after scattering, respectively. The last term,  $d\Delta'/d\Omega' = \sin\delta' d\delta'/\sin\theta' d\theta'$ , is the ion-frame scattering transfor-

mation which describes the deflection of the ejected electrons in the Coulomb field of the ion. In our classical model, this term has a singularity at  $\theta' = 0$  (i.e., in the direction of the focusing ion), which produces a strong enhancement in the differential cross section and gives rise to Coulomb focusing. The differential cross section prior to scattering,  $d\sigma/d\Delta$ , is assumed to be isotropic.

The predicted enhancement in the forward direction is accompanied by a small *deenhancement* for emission angles away from the focusing ion since the total electron emission cross section must be conserved. This deenhancement extends to backward angles but becomes unity at  $180^\circ$ . Coulomb focusing thus has a negligible effect upon those electrons emitted in the backward direction (i.e., away from the focusing ion). Therefore, target-to-projectile electron intensity ratios measured for symmetric low-energy collisions at extreme forward and backward emission angles should provide an accurate comparison with calculated enhancements due to Coulomb focusing.

Using this formulation, we have calculated the lifetime dependence of the Coulomb-focused differential cross section for target electron emission at  $0^\circ$  for 10-keV  $\text{He}^+ + \text{He}$  collisions. The differential cross section was obtained as a function of the lifetime  $\tau = 1/\Gamma$  through integration over the line shape of the doubly-differential cross section given in Eq. (1), for a fixed resonance energy of 33.3 eV corresponding to the  $2s^2^1S$  state. The theoretical lifetime-dependent enhancement, shown as the solid curve in Fig. 2, is the integrated Coulomb-focused differential cross section, scaled to agree with the  $2s^2^1S$  data point. The scaling was performed in lieu of explicitly taking into account the effects of the angular acceptance of the analyzer and the angular spreads associated with the incident and scattered ions, all of which affect the magnitude of the observed enhancement but are independent of lifetime. As can be seen, the lifetime dependence of the enhancement is described remarkably well by this simple calculation.

More detailed calculations have been performed of the angular dependence of the enhancement due to Coulomb focusing. These theoretical results have been compared

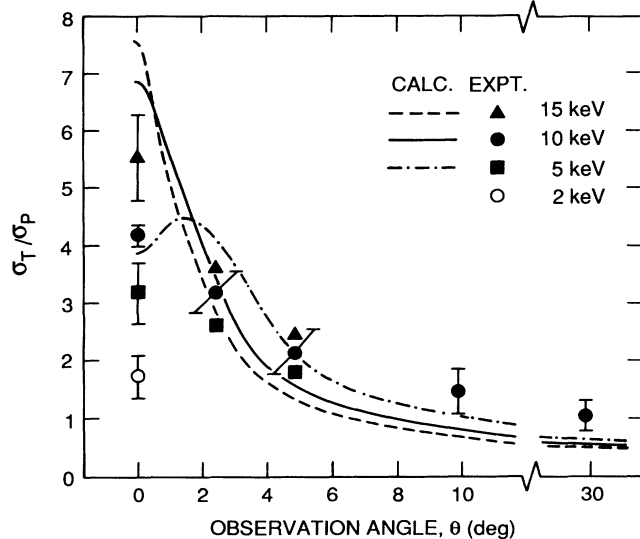


FIG. 3. Ratio  $\sigma_T/\sigma_P$  of total cross section for target electron emission,  $\sigma_T$ , and projectile emission,  $\sigma_P$ , plotted as a function of observation angle for four  $\text{He}^+ + \text{He}$  collision energies. The curves are the calculated angular dependence of the focused-to-unfocused differential cross-section ratio for the  $2s^2^1S$  state, determined using Eq. (1).

in Fig. 3 with measurements for 5, 10, and 15 keV. For these calculations we have convoluted the differential cross section derived from Eq. (1) with appropriate Gaussian distribution functions, which represent the energy-dependent small-angle scattering of the projectile ions during the collision,<sup>14</sup> and the 0.5° angular divergence of the incident beam. The resulting broadened focused differential cross section was then integrated over the 2.7° angular acceptance of the analyzer. The theoretical enhancement in the electron emission cross section is the ratio of the broadened Coulomb-focused differential cross section and the similarly "broadened" differential cross section obtained by setting  $d\Delta'/d\Omega'=1$ , which corresponds to the case where focusing does not occur. For simplicity, the calculation was done using the lifetime and resonance energy of the  $2s^2^1S$  state. We find excellent quantitative agreement at 10 keV between the calculated enhancement of 6.9 and the measured enhancement (see Fig. 2) of  $7.9 \pm 0.9$  for the  $2s^2^1S$  state at 0°. The present calculation is expected to overestimate the experimentally determined *total* target-to-projectile electron-emission cross-section ratio since the contributions of the other autoionizing states, which have significantly longer lifetimes, will tend to reduce the overall total enhancement. Nevertheless, our calculations reflect the general features of the measured angular and energy dependence of the total target-to-projectile enhancement quite satisfactorily.

On the basis of our theoretical model and the inversely proportional dependence of small-angle scattering of the  $\text{He}^+$  ion with collision energy, we expect the enhancement to become progressively more compressed about the incident beam direction as the energy increases above 15 keV. The magnitude of the enhancement is expected to reach a maximum value above which it decreases due to the strong collision energy dependence of the Coulomb focusing effect.

In summary, we have presented the first conclusive evidence for Coulomb focusing in low-energy  $\text{He}^+ + \text{He}$  collisions. Our time-dependent classical model of PCI satisfactorily describes the angular, lifetime, and projectile energy dependence of the effect (when angular scattering of the  $\text{He}^+$  projectile ion has been accounted for). We have shown that Coulomb focusing can produce order-of-magnitude enhancements in cross section for observation angles close to the ion-beam axis, and thus needs to be considered when measuring electron cross sections for such observation angles. Finally, it should be noted that the angular distribution of Coulomb-focused electrons reflect the angular scattering

of the projectile during the collision and thus may carry additional information about the production mechanisms leading to the doubly-excited states being populated.

We would like to thank C. Bottcher, J. Burgdörfer, R. Barrachina, and J. Macek for their interest in this problem and their many stimulating and insightful discussions. In addition, we are indebted to A. Bordenave-Montesquieu for illuminating and helpful comments and suggestions during the preparation of this manuscript. This work was supported by the Office of Fusion Energy, U.S. Department of Energy, under Contract No. DE-AC05-84OR21400 with Martin Marietta Energy Systems. J.K.S. was supported by Oak Ridge Associated Universities (ORAU). Support for N.S. and K.S. was provided through Nato Collaboration Grant No. 0194/87.

<sup>(a)</sup>Present address: University of Tennessee, Knoxville, TN 37996.

<sup>(b)</sup>Permanent address: Hahn-Meitner Institut für Kernforschung GmbH, Berlin, West Germany.

<sup>1</sup>R. B. Barker and H. W. Berry, *Phys. Rev.* **151**, 14 (1966).

<sup>2</sup>G. N. Ogurtsov, *J. Phys. B* **16**, L745 (1983).

<sup>3</sup>P. W. Arcuni, *Phys. Rev. A* **33**, 105 (1986).

<sup>4</sup>P. van der Straten and R. Morgenstern, *J. Phys. B* **19**, 1361 (1986).

<sup>5</sup>R. Morgenstern, A. Niehaus, and U. Thielmann, in *Proceedings of the Ninth International Conference on the Physics of Electronic and Atomic Collisions, Seattle, 1975, Abstracts of Contributed Papers*, edited by J. S. Risley *et al.* (University of Washington, Seattle, 1975).

<sup>6</sup>P. Dahl, M. Rødbro, B. Fastrup, and M. E. Rudd, *J. Phys. B* **9**, 1567 (1976).

<sup>7</sup>P. van der Straten, Ph.D. dissertation, Utrecht, 1987 (unpublished).

<sup>8</sup>M. G. Menendez, in *Proceedings of the Fifteenth International Conference on the Physics of Electronic and Atomic Collisions, Brighton, England, 1987*, edited by H. B. Gilbody *et al.* (North-Holland, Amsterdam, 1988).

<sup>9</sup>F. W. Meyer, C. C. Havener, R. A. Phaneuf, J. K. Swenson, S. M. Shafroth, and N. Stolterfoht, *Nucl. Instrum. Methods B* **24/25**, 106 (1987).

<sup>10</sup>M. Barat and W. Lichten, *Phys. Rev. A* **6**, 211 (1972).

<sup>11</sup>A. Bordenave-Montesquieu, A. Gleizes, and P. Benoit-Cattin, *Phys. Rev. A* **25**, 245 (1982).

<sup>12</sup>N. Stolterfoht, *Phys. Rep.* **146**, 317 (1987).

<sup>13</sup>W. Shearer-Izumi, *At. Data Nucl. Data Tables* **20**, 531 (1977).

<sup>14</sup>D. Bordenave-Montesquieu and R. Dagnac, *J. Phys. B* **12**, 1233 (1979).